Università degli Studi di Catania

SCUOLA SUPERIORE di CATANIA
MEDITERRANEAN UNIVERSITY CENTER

# Università degli Studi di Catania
# Scuola Superiore di Catania

International PhD

in

Stem Cells

XXIV

**Targeting Survival Pathways in Cancer Stem Cells**

**Marcello Maugeri-Saccà**

Coordinator of PhD

Prof. Daniele Condorelli

Co-tutor

Dr. Desiree Bonci

**Summary**

**Abstract**

**1) Introduction**

1.1 Clinical and Molecular Features of Breast Cancer

1.2 The "Cancer Stem Cells" Model

1.3 Breast Cancer Stem Cells

**2) Material and methods**

2.1 Isolation and cell cultures
2.2 Flow cytometry
2.3 Molecular Analysis
2.4 Colony forming ability assay
2.5 Western blot
2.6 Immunohistochemistry on tumor sections
2.7 Cell viability assays
2.8 Statistical analysis
2.9 Reverse Phase Phosphoprotein Microarrays (RPPM)
2.10 Gene expression profiling
2.11 Animal models

**3) Results**

3.1 *In vitro* characterization of breast cancer stem cells

3.2 Fetal bovine serum, but not retinoic acid, induced differentiation in breast cancer stem cells

3.3 Characterization of breast cancer stem cells through Reverse Phase Phosphoprotein Microarray

3.4 *In vivo* characterization of breast cancer stem cells: metastatic ability and metastatic pattern

3.5 Molecular profiling of differentiated breast cancer cells *vs* breast cancer stem cells *vs* metastatic breast cancer stem cells

3.6 Pattern of chemoresistance

**4) Discussion**

**5) References**

**6) Figures**

**Abstract**

The discovery of tumor-initiating cells endowed with stem-like features, and therefore referred to as cancer stem cells (CSCs), has added a further level of complexity to the pathobiology of neoplastic diseases. This uncommon cellular subpopulation has been connected with tumor initiation, metastatization and treatment failure. CSCs are protected against standard medical treatments by multiple mechanisms including the abnormal activation of both DNA damage repair signals and canonical survival pathways. Moreover, this cellular subset relies on dedicated signals such as self-renewal-linked molecular circuits. Therefore, the exact definition of the target population and the identification of molecular networks differentially activated in CSCs compared with their differentiated progeny are crucial for an optimal pre-clinical development of molecular targeted agents. We isolated breast CSCs from surgically resected primary breast tumors. A first round of experiments was designed in order to determine whether our clones met the operative criteria to be defined as CSCs. In particular, all these clones possessed: i) the expression of a unique repertoire of markers common to stem and progenitor cells, ii) an unlimited growth *in vitro* using media optimized for stem cell cultures and iii) the ability to reproduce the parental tumor upon injection in immunocompromised mice. Afterword, the metastatic potential of genetically engineered BCSCs was compared with that of differentiated breast cancer cells (dBCCs) . Upon both intracardiac and orthotopic injection the undifferentiated pool was able to generate distant metastases and to recapitulate the dissemination pattern of

the human disease, while dBCCs failed to generate distant lesions. Afterwards, high-throughput assays have been exploited in order to define molecular mechanisms underlying this differential metastatic proclivity. In particular, most up- and down-regulated genes were evaluated for their convergence on canonical signal pathways/biological functions. BCSCs displayed higher levels of DNA repair-linked effectors such as BRCA1, ATR, ATM and Chk1, higher level of the pro-tumorigenic and pro-metastatic protein c-MET and, finally, they were characterized by lower levels of physiological Wnt inhibitors (Dkk family members). Therefore, we identified three different pathways/functions whose hyper-activation seems to be correlated with the metastatic ability of BCSCs. Notably, molecular effectors of the above-mentioned pathways can be pharmacologically antagonized by experimental targeted agents.

# 1) Introduction

## 1.1 Clinical and Molecular Features of Breast Cancer

Although the mortality curves for many cancers remained quite stable over the past decades, major breakthroughs in translational oncology have opened new perspectives for the treatment of cancer. The advent of molecular targeted therapies has provided the proof-of-concept to selectively turn-off deregulated oncogenic proteins, while the identification and validation of predictive biomarkers of response has allowed to improve the performance of some targeted agents (1,2). Moreover, high-throughput biotechnologies capturing the molecular "fingerprints" of tumors have moved from a laboratory dimension to become part of clinical trails (3). Notwithstanding, breast cancer (BC) remains a significant public health concern, with more than a million new cases diagnosed annually. Prognosis and treatment of BC are largely dependent on clinical and pathological features including age, menopausal status, tumor size, grade, nodal involvement, hormonal receptors expression and HER-2 status. Given this heterogeneity it is not surprising that survival data revealed a wide variability in BC course, thus indicating that yet uncharacterized molecular differences are responsible for such heterogeneity. In recent years, whole genome profiling technologies offered a working model for BC molecular taxonomy. The original classification proposed by Perou, named "the molecular portrait of BC" (4), led to the identification of five subgroups (luminal A, luminal B, basal-like, HER2, and normal breast-like). Each group mainly differs for the presence or the absence of the estrogen receptor, the progesterone

receptor and the amplification/overexpression of the protoncogene Her2-neu. Moreover, the presence of germline BRCA1 mutations makes the picture even more complex since BRCA1-mutant BC are characterized by an early onset, an extremely aggressive biological behavior and a different spectrum of sensitivity to chemotherapy compared with all other subtypes (5). Given the growing availability of chemotherapeutic agents, hormonal manipulations and molecular targeted agents, an exact definition of molecular features of each BC subset is needed for sharpening the therapeutic potential of established and forthcoming drugs.

**1.2 The "Cancer Stem Cell" Model**

Growing evidence indicates that a cellular subpopulation with stem cell-like features, commonly referred to as cancer stem cells (CSCs), is critical for tumor generation and maintenance (6). This cellular fraction shares many properties with normal adult stem cells (SCs) and represents the prominent tumorigenic population able to propagate the parental tumor in animal models. CSCs are protected against widely used chemotherapeutic agents by means of different mechanisms such as proficiency in DNA damage repair and high expression of ATP-binding cassette drug transporters (7) (Fig. 1). Since it is reasonable to assume that long-lasting tumor regression can be achieved by an efficient target of this cellular population, an in-depth characterization of molecular mechanisms governing CSCs fate is a priority. The concept that a transformed stem cell is the progenitor of the entire tumor population implies that cancers are organized in a stringent hierarchy with a CSC at the apex of the pyramid

("hierarchical model"), in a distortion of the functional architecture of a normal tissue. Consistent with this hypothesis, increasing evidence suggests that CSCs aberrantly exploit molecules and pathways governing the self-renewal program (8), as indicated by the asymmetric distribution of self-renewal pathway effectors between CSCs and their differentiated offspring (9), and by the preferential depletion of the CSC pool following the pharmacological abrogation of self-renewal components (10). This population displays three operative characteristics that are currently adopted for isolation and characterization: **i)** expression of a repertoire of markers common to stem and progenitor cells, **ii)** unlimited growth *in vitro* using media optimized for stem cell cultures and **iii)** ability to reproduce the parental tumor upon injection in immunocompromised mice.

### 1.3 Breast Cancer Stem Cells

Breast CSCs (BCSCs) have been characterized by the immunophenotype $CD44^{+}/CD24^{low}/lin^{-}$, which defines a cellular subset accounting for 1% to 10% of the total population (11). BCSCs have been also isolated by the expression of ALDH1. Considering a partial overlap between the $CD44^{+}/CD24^{low}/lin^{-}$ and the ALDH1-positive population, as few as 20 cells $CD44^{+}/CD24^{low}/lin^{-}$ /ALDH1-positive are able to form a tumor (12). As discussed above, evidence indicates that CSCs aberrantly exploit self-renewal pathways. Consistent with this, the Notch, Hedgehog and Wnt pathways are thought to be important effectors whose aberrant activation sustains BCSCs behavior, while self-renewal pathway inhibitors are currently undergoing clinical trials (13). The abrogation of Notch activity through gamma-secretase inhibitors (GSIs) or a Notch 4-

neutralizing antibody significantly hampered mammosphere-forming ability in a model of ductal carcinoma *in situ* of the breast (14). Moreover, evidence indicates that Notch interacts with established and druggable oncogenic pathways such as the estrogen receptor and the Her2-neu pathways (15-17). To further enforce the connection between self-renewal pathways and BCSCs, it has been documented that the Hedgehog signal controls the self-renewal via the modulation of Bmi-1 (18), while the aberrant activation of the canonical WNT pathway conferred radioresistance to BCSCs (19). Notably, Akt neutralization sensitized BCSCs to radiotherapy via the inhibition of β-catenin.

BCSCs also appear to be endowed with an enhanced DNA repair ability. Transcriptional profiling of the putative CSC population isolated from the mammary gland of p53-null mice indicated that these cells were enriched in both DNA repair- and self-renewal-linked genes (20). Furthermore, mammospheres from the commercial cell line MCF-7 displayed a more active DNA single-strand break repair pathway in comparison to the bulk population (21), while long-term exposure of MCF-7/ADR cells to doxorubicin led to the gain of stem-like properties coupled with enhanced chemoresistance-conferring mechanisms (22). This is highlighted by an increased expression of genes encoding for multidrug resistance-related proteins and the cyclophosphamide-metabolizing enzyme aldehyde dehydrogenase 1. Radioresistance of BCSCs seems to be also due to lower concentrations of reactive oxygen species. This phenomenon is correlated with an increased expression of free radical scavenger systems, such as those belonging to the glutathione metabolism, which counteracts the effects of water radiolysis (23). This

radioresistant phenotype was reverted by the inhibition of glutathione metabolism, which restored BCSCs radiosensitivity and decreased their clonogenic potential.

Therefore, a deeper understanding of molecular pathways conferring chemoresistance properties and metastatic traits to BCSCs is a priority for optimal development of new molecular targeted agents within the hierarchical context of tumors.

## 2) Material and methods

### 2.1 Isolation and cell cultures

Breast cancer specimens were obtained upon informed consent from patients undergoing surgical resection according to the Institutional Ethical Committee guidelines on human experimentation and with the Helsinki Declaration. Briefly, surgical specimens dissociation was carried out by enzymatic digestion (20 mg/ml collagenase II, Gibco-Invitrogen, Carlsbad, CA) for 2 h at 37°C. Recovered cells were cultured at clonal density in serum-free medium supplemented with 20 mg/ml epidermal growth factor (EGF) and 10 mg/ml basic fibroblast growth factor (b-FGF) and Insulin (50 µg /ml). Flasks non-treated for tissue culture were used to reduce cell adherence and support growth as undifferentiated tumor spheres. The medium was replaced or supplemented with fresh growth factors twice a week until cells started to grow forming floating aggregates. Cultures were expanded by mechanical dissociation of spheres, followed by re-plating of both single cells and residual small aggregates in complete fresh medium. To obtain differentiation of breast cancer sphere-forming cells, stem cell medium was replaced with DMEM supplemented with 10% serum or Retinoic Acid 10 µM (RA) in culture-treated flasks, to allow cell attachment and differentiation. The acquisition of differentiation markers was evaluated by FACS staining.

### 2.2 Flow cytometry

For flow cytometry, tumor spheres and differentiated counterparts were dissociated as single cells, washed and incubated with the appropriate dilution of control or specific antibody. Antibodies used were APC-conjugated anti-CD44, PE/Cy7-conjugated anti-CD24 from Biolegend (San Diego, CA) anti-CK18 and anti-CK14 both from Millipore (Billerica, MA). After 45 min incubation, cells were washed or, where necessary, incubated with FITC- or PE-conjugated secondary antibodies for 30 min. and washed again before analysis using either a FACScan or an LSRII flow cytometer (Becton Dickinson).

### 2.3 Molecular Analysis

Mutational screening was performed on the coding exons 5 to 8 of *TP53*. Genomic DNA specimens were obtained from BCSCs using PureLinkTM Genomic DNA Purification Kit (Invitrogen, Carlsbad, CA) according to the manufacturer's protocols. Total RNA was extracted from BCSCs using the RNeasy mini kit (Qiagen, Hilden, Germany). RNA (1µg) was reverse transcribed into cDNA by using SuperScript II RT with oligo(dT) as primers (Invitrogen) according to the manufacturer's protocol. PCR amplifications were carried out using high-fidelity Optimase polymerase (Transgenomic, Omaha, NE).

**2.4 Colony forming ability assay**

Soft agar colony forming assays were carried out for untreated BCSCs. Briefly, cells were washed and 500 single cells were plated in the top agar layer in each well of a 24-well culture plate with 0.3% top agar layer and 0.4% bottom agar layer (SeaPlaque Agarose, Cambrex, NJ). Cultures were incubated at 37°C for 20 days. Colonies from triplicate wells were stained with crystal violet (0.01% in 10% MetOH), visualized and counted under microscope and, afterwards, photographed and sorted with a FACS Aria (Becton Dickinson).

**2.5 Western blot**

Whole cell lysates (20µg) from BCSCs and differentiated counterparts were fractioned on SDS-polyacrylamide gels, blotted to nitrocellulose membranes and incubated with the following antibodies: CK14 and CK18 from Millipore (Billerica, MA), phosphorylated Chk1 (Ser345) from Cell Signaling Technology (Danvers, MA, USA); α-nucleolin from Santa Cruz Biotecnology (Santa Cruz, CA) was used as loading control.

**2.6 Immunohistochemistry on tumor sections**

Immunohistochemistry was performed on formalin-fixed, paraffin-embedded or frozen tissue. Paraffin sections (5 µm) were dewaxed in xylene and rehydrated with distilled water. Sections were treated with heat-induced epitope retrieval technique using a citrate buffer (pH 6). For PanCKs detection, epitope retrieval technique was based on EDTA

(pH 8). After peroxidase inhibition with 3% H2O2 for 20 min, the slides were incubated with low and medium molecular weight CKs (DakoCytomation). The reaction was performed using Elite Vector Stain ABC systems (Vector Laboratories) and DAB substrate chromogen (DakoCytomation), followed by counterstaining with haematoxylin.

**2.7 Cell viability assays**

For cell viability studies, dissociated spheres, differentiated cells and xenograft-derived (primary and metastatic) cells were plated in 96-well plates at 3.000 cells/well in growth medium supplemented with doxorubicin (15ng/ml) or paclitaxel (5ng/ml), for 72-96h. Cell viability was evaluated by CellTiter-Glo Luminescent Cell Viability Assay (Promega, Madison, WI) according to standard protocols and analyzed with a Victor 2 plate reader (Wallac, Turku, Finland).

**2.8 Statistical analysis**

All statistical analyses were performed using GraphPad Prism 4 (GraphPad Software Inc., www.graphpad.com). Data are presented as mean ± standard deviation (SD). Statistical significance was determined by two-way ANOVA with Bonferroni post-test.

**2.9 Reverse Phase Phosphoprotein Microarrays (RPPM)**

RPPM were printed with whole breast stem and differentiated cancer cell lysates in triplicate spots. Briefly, the cells were collected from their cultures, washed in PBS (Invitrogen, Carlsbad, CA) and then lysed with a T-PER-based (Thermo Fisher Scientific, Waltham, MA) lysis buffer. Cell lysate concentrations were measured using a

Spectrophotometer (Eppendorf, Hamburg, Germany) in a solution containing 1µl of cell lysates in a 50% of borate buffer saline preparation and a 50% of Coomassie protein assay reagent (Thermo Fisher Scientific, Waltham, MA). Cell lysates were then diluted in an extraction buffer containing 50% T-PER (Thermo Fisher Scientific, Waltham, MA), 47.5% 2xSDS (Invitrogen, Carlsbad, CA) and 2.5% β-mercaptoethanol (Thermo Fisher Scientific, Waltham, MA) to have a printing concentration of 0.25µg/µl. They were printed on glass-backed nitrocellulose array slides (GRACE Bio-Labs, Bend, OR) using an Aushon 2470 arrayer equipped with 185-µm pins (Aushon Biosystems, Billerica, MA). Together with the samples, array calibrator lysates, such as HeLa + Pervanadate (BD, Franklin Lakes, NJ), Jurkat + Etoposide (Cell Signaling, Danvers, MA) and Jurkat + Calyculin A (Cell Signaling, Danvers, MA), were printed in a 10-points dilution curve as positive controls. Each calibrator was printed in triplicate spots in double concentrations of 0.5µg/µl and 0.125µg/µl. At the end of the printing run, selected printed slides were stained with Sypro Ruby Protein Blot Stain (Invitrogen, Carlsbad, CA) to estimate sample total protein concentration, and the left slides were directly stored at -20°C. Prior antibody staining, printed slides were treated with 1x ReBlot Mild Solution (Chemicon, Temecula, CA), washed 2x5min with 1xPBS (Invitrogen, Carlsbad, CA) and incubated for 1 hour in blocking solution (I-Block, Applied Biosystems, Foster City, CA).They were then probed with a library of 166 anti-total, -cleaved and -phospho-protein antibodies with DAKO automated stainer (according to the manufacturer's instructions) using Catalyzed Signal Amplification

System kits (DAKO, Carpinteria, CA) and protein detection was performed with streptavidin-conjugated IRDye680 (Li-COR Bioscience, Lincoln, NE) fluorophore. Primary antibodies were validated prior to use by immunoblotting with complex cellular lysates, such as commercial cell lysates or human tissue lysates. The negative control slides were incubated with an antibody diluent (Dako, Carpinteria, CA). Secondary antibody was goat anti-rabbit IgG heavy + light (1:7500) (Vector Laboratories, Burlingame, CA) or rabbit anti-mouse IgG (1:10) (Dako, Carpinteria, CA). All Sypro and immunostained slides were scanned using a Revolution 4550 scanner (Vidar Corp., Herndon, VA) and acquired images were analyzed with MicroVigene v4.0.0.0 (VigeneTech, Carlisle, MA) that performed spot detection, local background subtraction, negative control subtraction, replicate averaging and total protein normalization, producing a single value for each spot/sample. Unsupervised hierachical clusterings were performed with Jump v5.1 (SAS Institute, Cary, NC); endpoint relative intensity plots were performed with GraphPad Prism 5 (GraphPad Software Inc., Avenida de la Playa La Jolla, CA). Statistical analysis was performed on RPMM relative intensity values using R version 2.9 software (R Development Core Team, Vienna, Austria). Initially, the distribution of variables was checked. If the distribution of variables for the analyzed groups was normal, a two-sample t-test was performed. If the variances of two groups were equal, two-sample t-test with a pooled variance procedure was used to compare the means of intensity between two groups. Otherwise, two-sample t-test without a pooled variance procedure was adopted. For non-normally

distributed variables, the Wilcoxon rank sum test was used. All significance levels were set at $p < 0.05$.

**2.10 Gene expression profiling**

Transcriptomic analysis of BCSC was performed with the Affymetrix Human Exon 1.0 ST Array, which provides an accurate picture of gene expression covering the whole transcriptome. Raw data files were normalized according to the RMA method by the BRB Array tools plugin for Microsoft Excel using the appropriate statistic tools for detecting significant changes in gene expression.

**2.11 Animal models**

For *in vivo* tracking, cells were transfected with lentiviral vector encoding luciferase/enhanced green fluorescent protein (Luc/EGFP -breast cancer stem cells -) or luciferase/red fluorescent protein (Luc/RFP -differentiated cells-) reporter gene and injected either intracardiacally or in the mammary fat pad alone or in defined ratios (Patent application number: 20100016406, IPC8 Class: AA61K317088FI, USPC Class: 514 44A). For performing the latter surgical technique, mice were anesthetized using a mixture of ketamine and xilazine (100 mg/Kg and 10 mg/Kg, respectively) and a short opening was made near the inguinal nipples. After removing the mouse epithelial compartment of the mammary gland, a total of 10.000 cells were slowly injected in the mammary fat pad using a 29G needle; incision was closed using surgical staples, and 1 mL of warm PBS was injected subcutaneously. Bioluminescence imaging was performed to assess the growth rate of orthotopic model and the onset of distant

metastases. To do this, mice were intraperitoneally injected with luciferin (150 mg/kg) approximately 10 minutes before imaging, and a cryogenically cooled imaging system (IVIS 100 Imaging System, Xenogen) was used for whole body imaging. Signal intensities were quantified as the sum of all detected photons (Living Image Software 2.50). Mouse were then sacrificed, and organ explants was made in correspondence of bioluminescent signals; explanted organs were then analyzed under a stereomicroscope (Olympus SZX10) equipped with a fluorescence unit, allowing to discriminate RFP positive and EGFP positive cells (supported by a grant from the Italian Ministry of Health, oncology program Italy-USA. "Control of prostate cancer progression by microRNA-15 and -16". Fasc.527D, 2009-2012).

## 3) Results

### 3.1 *In vitro* characterization of breast cancer stem cells

Six BCSC clones have been isolated after surgical removal of primary ductal or lobular carcinoma of the breast. Standard molecular features, including tumor histology, estrogen receptor status, progesterone receptor status and HER-2 overexpression/amplification, were available (Table1). The first round of experiments was designed in order to characterize our clones and, in particular, whether these clones encompassed the operative criteria generally adopted for defining CSCs. The clonogenic assay documented the presence of cells endowed with self-renewal ability, with an overall percentage that was consistent with the relative abundance of CSCs in breast cancer (Fig.2 panel A). The stem-like immunophenotype $CD44^{+}CD24^{low}$ was confirmed with FACS analysis, with the exception of the 308 cell line that was highly positive for the $CD44^{+}CD24^{+}$ profile (Fig.2 panel B).

We previously documented that lung CSCs activate Chk1 when exposed to standard of care chemotherapeutic agents such cisplatin and taxanes (24). While the aberrant activation of G2-M checkpoint controllers conferred chemoresistance, the pharmacological inhibition of Chk1 significantly increased chemosensitivity by triggering a modality of cell death known as mitotic catastrophe. The logic behind the development of Chk1 inhibitors is a modality of gene-gene interaction known as synthetic lethality (25). According with this model, while a mutation confers an advantage for cancer cells, the concomitant pharmacological abrogation of a redundant

pathway significantly affects cell fitness. Since p53-defective cells are unable to undergo G1 arrest, they depend on alternative checkpoint activators to arrest the cell cycle in response to DNA damages. Based on this premise, we assessed the p-53 status and, with the exception of the 308 cell line, all clones displayed wild-type p-53(Fig.2 panel C).

**3.2 Fetal bovine serum, but not retinoic acid, induced differentiation in breast cancer stem cells**

Since the primary endpoint of the project was to determine differential and targetable pathways activated in BCSCs compared with their differentiated offspring, optimal definition of differentiation protocols was introductory before performing high-throughput assays. To this end, a direct comparison of two protocols was carried out. In doing so, we compared standard fetal bovine serum-based (FBS) differentiation with retinoic acid-mediated differentiation (RA). In the clinical setting, the sequential use of differentiating agents and chemotherapy has shown considerable efficacy in acute promyelocytic leukemia (26) and, more recently, a randomized phase II trial demonstrated an increased response rate in non-small cell lung cancer patients when all-*trans* retinoic acid was associated with platinum-containing therapy (27). Moreover, brain tumor-derived CSCs exposed to RA underwent both growth arrest and expression of lineage-specific differentiation markers (28). Notwithstanding, the exposition to different concentration of (RA) failed to differentiate BCSCs, while exposition to (FBS) resulted in the expression of the myoepithelial cytokeratin 14 (CK14), coupled with

increased expression of the luminal CK18 in the BC308 clone. Successful differentiation was confirmed by fluorescence-activated cell sorting (FACS) analysis (Fig. 3).

**3.3 Characterization of breast cancer stem cells through Reverse Phase Phosphoprotein Microarray**

Given the complexity and heterogeneity of genetic derangements, cancer is canonically defined as a "genetic disease". Although microarray analysis of gene expression patterns has provided a way to improve diagnosis and risk stratification, these tools offer an incomplete picture of protein-protein interactions. Recent data showed that the multitude of genetic changes found in tumors functionally deregulate a limited number of cellular pathways. Therefore, proteomic analysis allows the detection of aberrant protein circuits (29). Among technologies developed for this purpose, reverse-phase protein microarray (RPPM) allows a rapid identification of aberrant pathways in small-volume samples.

Once established optimal criteria for stem cell differentiation, RPPM analysis was performed in order to detect asymmetry in deregulated pathway nodes/biological functions between BCSCs and differentiated breast cancer cells (dBCCs) (collaboration with Prof. L. Liotta and Prof. E. Petricoin, co-directors of the Center for Applied Proteomics at George Mason University, Manassas, VA). In doing so, we took advantage of a panel of 166 anti-total, -cleaved and -phospho-protein validated antibodies, able to recognize a wide range of molecular endpoints implicated in a variety of biological functions spanning from mitogenic signals to DNA repair and apoptotic pathways. As showed in the "heat map", phosphoprotein profiles of BCSCs clustered

together, to a similar extent to which dBCCs displayed a comparable phosphoprotein profile (Fig. 4). Afterward, we sought to determine most activated endpoints in BCSCs compared with their differentiated progeny. While dBCCs preferentially activated cell cycle-related proliferative signals (Cyclin B1, pAurora A, p-4E-BP1) and mitogenic intracellular effectors (p-ERK and p-p70 S6 Kinase), BCSCs expressed higher levels of pro-migratory factors such as Cox-2 (Fig. 5). This different distribution of cell cycle controllers is consistent with a more quiescent/slow proliferative behavior of CSCs, a functional property that has been connected with chemo-radioresistance (7).

**3.4 *In vivo* characterization of breast cancer stem cells: metastatic ability and metastatic pattern**

As discussed above, operative criteria for defining CSCs also include their ability to reproduce a phenocopy of the parental tumor upon injection in immunocompromised mice. To this end, two different models have been exploited. Firstly, the metastatic rate of BCSCs and dBCCs was determined upon intracardiac injection. To do this, mice (N=4/group) were inoculated with luciferase-infected and fluorescent-labeled BCSCs, dBCCs or both (at a defined ratio of 1:1), as discussed in the material and methods section. Bioluminescence signals became evident only in BCSC-injected mice and, after explants of target organs (liver, bones), only green spots were detectable. This indicated that stem-like cells represent the only population able to generate lesions in animal models (Fig. 6). However, one of the main limitations in preclinical research is the lack of reliable animal models able to recapitulate the natural course of human cancers.

Although intracardiac injection is currently used for determining the metastatic ability of cancer cells, this model provides only a partial picture of the metastatic cascade. In fact, tumor metastases result from a coordinate series of events, which include, at the primary site, extracellular matrix invasion, neoangiogenesis and ability to gain access to the circulatory system. To overcome this drawback BCSCs, dBCCs and a combination of BCSCs and dBCCs have been injected into orthotopic sites. In such a manner it is possible i) to reproduce the whole sequence of events through which primary cancer cells give raise to distant lesions, ii) to realize a close simulation of the natural course of human cancers and iii) to simulate all therapeutic settings, from the (neo)adjuvant to the adjuvant and metastatic setting. BCSCs and dBCCs were differentially transduced with lentiviral vectors coding for green and red reporter protein, respectively, mixed in a defined ratio (BCSCs:dBCCs =1:1 ) and inoculated into mice mammary fat pad. Three or four weeks later the mammary gland was surgically removed in order to simulate the surgical treatment of human breast cancer. The BCSCs was the only population able to migrate and to give raise to distant metastases (total N. of mice/N. of metastatic mice =12/9). Moreover, BCSCs recapitulated the pattern of human metastatic disease being the lung and nodes the most common sites of distant lesions (Fig. 7). It is known that the interplay between CSCs and the microenvironment is a dynamic process leading to the continuous remodeling of both compartments. Experimental evidence confirms the critical role of the epithelial-mesenchymal transition (EMT) in the development of cancer metastases and chemoresistance. Recent findings have demonstrated that EMT is

induced by the activation of a transcriptional complex influenced by different paracrine-acting signals, including the self-renewal-associated pathways Hedgehog (30), Notch (31) and Wnt (32). This complex leads to radical cytoskeletal rearrangements culminating in a switch toward a mesenchymal-like phenotype, pictured by the E-cadherin to N-cadherin switch. Cells undergoing these morpho-functional changes are typically located at the tumor-stroma interface, where they gain pro-metastatic traits coupled with increased clonogenicity and enrichment in stem cell-associated markers (33). We detected an increased expression, at a protein level, of N-cadherin in metastatic BCSCs compared with the mammary fat pad-injected BCSCs, while an opposite trend was seen for E-cadherin expression (Fig. 8). This observation implies that the orthotopic model allows a reliable simulation of the metastatic cascade, which also include the EMT. Finally, when metastatic BCSCs (mBCSCs) were harvested and re-injected into the murine background a shortening time to engraftment has been observed (Table 2), thus indicating that additional molecular changes occur in BCSCs during the metastatic cascade.

### 3.5 Molecular profiling of differentiated breast cancer cells *vs* breast cancer stem cells *vs* metastatic breast cancer stem cells

Given the aggressiveness gradient (dBCCs vs BCSCs vs mBCSCs) documented after *in vivo* experiments, gene expression profiling have been adopted to determine molecular circuits underpinning such biological differences. Given the expanding pipeline of inhibitors approved for clinical use or in late phases of clinical development, we

evaluated most up-or down-regulated genes according with their convergence of targetable pathways. To this end, public available algorithms such as Ingenuity Pathways Analysis (IPA) and the KEGG pathway database have been exploited for a pathway-focused elaboration of microarray data. With this approach whole pathways/biological functions have been explored. More in detail, we evaluated canonical survival pathways including: the epidermal growth factor receptor family, the insulin-like growth factor receptor pathway, the platelet-derived growth factor receptor signaling, the transforming growth factor beta pathway and the fibroblast growth factor receptor pathway. To a similar extent apoptotic signals, DNA damage sensor and repair pathways, cell cycle checkpoints and self-renewal-related pathways have been thoroughly examined. By taking advantage of this approach we detected a marked activation of the G2-M checkpoint in BCSCs compared with their offspring, as documented by increased level of Chk1, ATR and ATM (Fig. 9a), with increased levels of activated Chk1 confirmed by Western blot analysis (Fig. 9b). The ATM-Chk1 axis is a master controller of cell cycle checkpoints and is engaged under replication stresses or consequently to double-strand breaks. While this system avoid that cells acquire transforming mutations, cancer cells improperly activate DNA repair pathways to survive chemotherapy (7). To a similar extent BCSCs over-expressed the hepatocyte growth factor receptor (c-Met), a well-established oncogenic pathway associated with the development of distant metastases (Fig. 9c), with differential c-MET levels confirmed by FACS analysis (Fig. 9d). As discussed above, it is generally accepted that

CSCs rely on dedicated pathways, functionally interconnected with their ability to self-renew. Here, we found that BCSCs also present lower levels of physiological Wnt pathway inhibitors belonging to the DKK family (DKK1 and DKK3), compared to dBCCs (Fig. 9e). This finding suggests that BCSCs aberrantly use the Wnt signal transduction pathway that, in turn, could be connected with both "stemness" maintenance and metastatic proclivity. When considering CSCs markers, tumors arising from BCSCs displayed lower levels of CD24 than tumors generating with more differentiated cells, although no substantial differences were observed for others known (CD44, ALDH1) or putative (SOX2,OCT3/4, Nanog) stem cell markers(Fig. 9f).

### 3.6 Pattern of chemoresistance: dBCCs *vs* BCSCs *vs* metastatic BCSCs

One of the main implications of the CSC model is that this cellular subset is protected against standard medical treatment by means of multiple mechanisms including proficiency in DNA damage repair and altered cell cycle kinetics. Moreover, CSC-extrinsic mechanisms of drug resistance have been described, such as the induction of EMT or hypoxia (7). Given that the aberrant activation of G2-M checkpoint effectors and EMT-related pathways has been connected with chemoresistance, a chemosensitivity assay has been performed. As expected, BCSCs were more resistant of dBCCs to doxorubicin (Fig. 10) and, although to a lesser extent, to paclitaxel (data not shown), two chemotherapeutic agent commonly used for treating both early and advanced breast cancer. In turn, BCSCs harvested from metastatic lesions displayed enhanced chemoresistance compared to BCSCs harvested form the site of orthotopic

injection. Therefore, these data confirm the chemoresistant nature of CSCs and, even more important, suggest that BCSCs become chemorefractory during the metastatic progression. This different degree of responsiveness to chemotherapy could explain, in turn, the pattern of disease progression during sequential chemotherapeutic regimens.

## 4) Discussion

Mounting evidence points to CSCs as responsible for tumor generation and treatment failure. Therefore, the exact definition of the target population is crucial for an optimal pre-clinical development of molecular targeted agents and for achieving long-lasting tumor remission. In recent years, the advent of high-throughput biotechnologies is providing an unprecedented level of resolution about molecular mechanisms governing cancer cells, while the possibility to easily expand *in vitro* CSCs is allowing studying the molecular fingerprint of tumor within a hierarchical context.

Here, we took advantage of array-based gene expression analysis coupled with RPPM in order to capture a snapshot of deregulated genes/proteins in BCSCs compared with their non-tumorigenic offspring. Given that optimal quality controls are needed for sharpening the potential of high-throughput assays, we successfully established a differentiation protocol by comparing FBS and RA. Our data clearly indicate that FBS, as opposed to RA, successfully differentiated BCSCs.

Although our clones, when evaluated *in vitro*, possessed the general features of CSCs, the ability to produce a phenocopy of the parental tumor upon injection into the murine background is the hallmark for defining the CSC pool. Moreover, given the possibility to expand CSCs *in vitro*, the generation of CSC-based tumor xenografts is now considered as the gold standard for evaluating the anti-cancer properties of experimental agents (34). This is because of commercial cancer cell lines, which have been traditionally used for generating tumors in mice, are unable to give raise to a tumor

resembling the human disease. In the first round of *in vivo* experiments we found that BCSCs, but not dBCCs, were able to generate lesions upon intracardiac injection and, even more important, BCSCs recapitulated the metastatic pattern of the human disease. Although intracardiac injection is widely used for determining the metastatic ability of cancer cells, this model provides only a partial picture of the metastatic cascade and, therefore, it cannot be considered as a simulation of the human disease. Conversely, it is extremely likely that the orthotopic transplantation of CSCs will allow more reliable testing of anti-cancer agents by taking into account each therapeutic setting, from the (neo)adjuvant to the metastatic setting. In order to address this question, genetically engineered BCSCs and dBCCs were injected in the mammary fat pad either alone or combined in a defined ratio. The BCSCs was the only population able to migrate and to give raise to distant metastases, with the distant spread that recapitulated the metastatization pattern of human breast cancer, as documented by the presence of pulmonary and lymph node metastases.

In recent years, many attempts have been made for dissecting molecular signals associated with the onset of breast cancer metastases. The introduction of whole genome profiling technologies has expanded our knowledge of the genetic pathways associated with the development and progression of cancer and, more recently, microarray analysis of gene expression profiles has provided a way to improve diagnosis and risk stratification of cancer patients. Two prognostic signatures, for instance, the MammaPrint® (3) and the Oncotype DX® (35), have been validated in breast cancer and

represent the basis for large ongoing clinical trials named MINDACT (Microarray In Node negative Disease may Avoid ChemoTherapy) and TAILORx (Trial Assigning Individualized Options for Treatment). However, it is still unclear the relevance of single pathway on breast cancer metastatization, especially when considered within the pyramidal organization of tumors.

By taking advantage of gene expression profiling we documented an *in vivo* aggressiveness pattern (dBCCs < BCSCs < mBCSCs) that was sustained by the hyper-activation of master oncogenic signals including the G2-M checkpoint and the c-MET and Wnt pathways. It is worth noting that anti-Chk1 and anti-Met inhibitors are currently undergoing clinical trials. For instance, c-MET inhibition has been linked with an unprecedented bone metastasis response rate in patients with advanced prostate cancer (36), and a promising antitumor activity has been reported in non-small cell lung cancer patients whose tumors harbor KRAS mutations (37).

When considering Chk1 as a target for anti-cancer therapy, many Chk1 inhibitors demonstrated chemosensitizing properties in the preclinical setting and are undergoing early phases of clinical development (38). Notwithstanding, two main concerns recently arose from preclinical evidence and early clinical data. Firstly, the preferential antitumor activity of Chk1 inhibitors against p53-defective cells has been questioned (39). Secondly, although Chk1 antagonists were thought to have a favorable therapeutic index, two phase I dose-escalation trials with AZD7762 reported an unexpected

cardiotoxicity (40,41), and cardiac dose-limiting toxicity was also observed with the Chk1 inhibitor SCH 900776 (42).

Different compounds able to directly or indirectly antagonize the Wnt pathway have been synthesized and are in late preclinical development (43). Therefore, our data provide a defined working model for testing these compounds in a disease-oriented manner and within the hierarchical organization of breast cancer.

We also documented increased levels of N-cadherin in metastatic BCSCs compared with mammary fat pad-injected BCSCs. This suggests that the occurrence of EMT enables BCSCs to give raise to distant metastases. The EMT phenotype is induced by a transcriptional complex whose activation is driven by both canonical paracrine-acting pathways (TGF-β) and "stemness"-associated signals (Hedgehog, Notch and Wnt pathways) (44). Therefore, experimental compounds able to antagonize these pathways could be evaluated as perioperative therapy for preventing both the gain of a stem-like state and the acquisition of metastatic ability.

We also exploited RPPM analysis in order to detect dysfunctional pathway nodes in our CSC model. While dBCCs displayed higher level of pro-survival proteins and cell cycle-related proliferative signals, BCSCs were characterized by higher levels of migration-related proteins. This is consistent with experimental evidence showing that prolonged exit from the cell cycle is a hallmark of stem cells, representing a mechanism that ensures them longevity by preventing the exhaustion of the replicative potential (45). Label-retaining approaches indicated that CSCs exhibit similar slow proliferation

kinetics and, as a consequence, they are mostly spared by chemotherapy-induced death stimuli. For instance, ovarian and pancreatic cancer label-retaining population, both encompassing the operative criteria to be defined as CSCs, were able to survive, unlike non-label-retaining cells, to standard chemotherapeutic agents such as cisplatinum and 5-fluorouracil, respectively (46,47).

Finally, our BCSC displayed a chemoresistant phenotype, a feature that became more evident with the increased metastatic potential. Therefore, the development of chemotherapy-enhancing agents aimed at eliminating CSCs must be considered a priority, even though safety issues correlated with "off-target effects" on tissue-resident stem cells must be taken into account in order to avoid toxicity-related discontinuation of clinical trials.

To sum up, our data clearly indicate the crucial role of BCSCs in the generation of cancer metastases. Moreover, our *in vivo* model is a simulation of human breast cancer that we are exploiting for testing molecular targeted agents direct against deregulated BCSC pathways.

## 5) References

1) Slamon DJ, Leyland-Jones B, Shak S, et al. Use of chemotherapy plus a monoclonal antibody against HER2 for metastatic breast cancer that overexpresses HER2. *N Engl J Med* 2001;344(11):783-792.

2) Rosell R, Moran T, Queralt C et al. Screening for Epidermal Growth Factor Receptor Mutations in Lung Cancer. *N Engl J Med* 2009;361(10):958-967.

3) Cardoso F, Van't Veer L, Rutgers E, et al. Clinical application of the 70-gene profile: the MINDACT trial. *J. Clin. Oncol.* 2008;26:729-735.

4) Perou CM, Sørlie T, Eisen MB, et al. Molecular portraits of human breast tumours. *Nature.* 2000;406(6797):747-52.

5) Vollebergh MA, Jonkers J, Linn SC. *Cell Mol. Life Sci*. 2011. Genomic instability in breast and ovarian cancers: translation into clinical predictive biomarkers.

[Epub ahead of print]

6) Saini V and Shoemaker RH.Potential for therapeutic targeting of tumor stem cells. *Cancer Sci* 2010;101(1):16-21.

7) Maugeri-Saccà M, Vigneri P and De Maria R. Cancer Stem Cells and Chemosensitivity. *Clin. Canc. Res.* 2011;17(15):4942-7.

8) Maugeri-Saccà M, Zeuner A and De Maria R. Therapeutic Targeting of Cancer Stem Cells. *Front. Oncol. 2011*;1:10.

9) Peacock CD, Wang Q, Gesell GS, et al. Hedgehog signaling maintains a tumor stem cell compartment in multiple myeloma. *Proc. Natl. Acad. Sci. U S A* 2007;104:4048-4053.

10) Bar EE, Chaudhry A, Lin A, et al. Cyclopamine-mediated Hedgehog pathway inhibition depletes stem-like cancer cells in glioblastoma. *Stem Cells* 2007;25:2524-2533.

11) Al-Hajj M, Wicha MS, Benito-Hernandez A et al. Prospective identification of tumorigenic breast cancer cells. *Proc Natl Acad Sci U S A* 2003;100:3983-3988.

12) Ginestier C, Hur M, Charafe-Jauffret E, et al ALDH1 is a marker of normal and malignant breast stem cells and a predictor of poor clinical outcome. *Cell Stem Cell* 2007; 1:555-557.

13) Von Hoff DD, LoRusso PM, Rudin CM, Reddy JC, Yauch RL, Tibes R, et al. Inhibition of the hedgehog pathway in advanced basal-cell carcinoma. *N. Engl. J. Med.* 2009;361:1164-1172.

14) Farnie G, Clarke RB, Spence K, et al. Novel cell culture technique for primary ductal carcinoma in situ: role of Notch and epidermal growth factor receptor signaling pathways. *J. Natl. Cancer Inst.* 2007;99:616–27.

15) Korkaya, H and Wicha MS. HER-2, notch, and breast cancer stem cells: targeting an axis of evil. *Clin. Cancer Res*. 2009;15:1845-1847.

16) Cicalese A, Bonizzi G, Pasi CE, et al. The tumor suppressor p53 regulates polarity of self-renewing divisions in mammary stem cells. *Cell*. 2009;138:1083-1095.

17) Magnifico A, Albano L, Campaner S, et al Tumour-initiating cells of HER2-positive carcinoma cell lines express the highest oncoprotein levels and are trastuzumab sensitive. *Clin. Cancer Res*. 2009;15**:**2010–2021.

18) Liu S, Dontu G, Mantle ID, et al. Hedgehog signaling and Bmi-1 regulate self-renewal of normal and malignant human mammary stem cells. *Cancer Res.* 2006;66: 6063-6071.

19) Zhang M, Atkinson RL, Rosen JM. Selective targeting of radiation-resistant tumor-initiating cells. *Proc. Natl. Acad. Sci. USA* 2010;107:3522-3527.

20) Zhang M, Behbod F, Atkinson RL, Landis MD, Kittrell F, Edwards D, et al. Identification of tumor-initiating cells in a p53-null mouse model of breast cancer. *Cancer Res.* 2008;68:4674-4682.

21) Karimi-Busheri F, Rasouli-Nia A, Mackey JR, Weinfeld M. Senescence evasion by MCF-7 human breast tumor-initiating cells. *Breast Cancer Res*. 2010;12:R31.

22) Calcagno AM, Salcido CD, Gillet JP, et al. Prolonged drug selection of breast cancer cells and enrichment of cancer stem cell characteristics. *J. Natl. Cancer Inst.* 2010;102:1637-1652.

23) Diehn M, Cho RW, Lobo NA, et al. Association of reactive oxygen species levels and radioresistance in cancer stem cells. *Nature* 2009;458:780-783.

24) Bartucci M, Svensson S, Romania P, et al. Therapeutic targeting of Chk1 in NSCLC stem cells during chemotherapy. Cell Death Differ. 2011 [Epub ahead of print]

25) Ashworth A, Lord CJ, Reis-Filho JS. Genetic interactions in cancer progression and treatment. *Cell.* 2011;145:30-38.

26) Sanz MA, Martin G, Gonzalez M, et al. Risk-adapted treatment of acute promyelocytic leukemia with all-*trans*-retinoic acid and anthracycline monochemotherapy: a multicenter study by the PETHEMA group. *Blood* 2004;103: 1237-1243.

27) Arrieta O, González-De la Rosa CH, Aréchaga-Ocampo E, et al. Randomized phase II trial of All-trans-retinoic acid with chemotherapy based on paclitaxel and cisplatin as first-line treatment in patients with advanced non-small-cell lung cancer. *J. Clin. Oncol.* 2010;28:3463-3471.

28) Yin M, Wang S, Sang Y, *et al*. Regulation of glioblastoma stem cells by retinoic acid: role for Notch pathway inhibition. *Oncogene* 2011. [Epub ahead of print].

29) Mueller C, Liotta LA, Espina V. Reverse phase protein microarrays advance to use in clinical trials. *Mol. Oncol.* 2010;4:461-481.

30) Ohta H, Aoyagi K, Fukaya M, *et al*. Cross talk between hedgehog and epithelial-mesenchymal transition pathways in gastric pit cells and in diffuse-type gastric cancers. *Br. J. Cancer* 2009;100:389-398.

31) Wang Z, Li Y, Kong D, *et al.* Acquisition of epithelial-mesenchymal transition phenotype of gemcitabine-resistant pancreatic cancer cells is linked with activation of the notch signaling pathway. *Cancer Res*. 2009;69:2400-2407.

32) Gupta S, Iljin K, Sara H, *et al.* FZD4 as a mediator of ERG oncogene-induced WNT signaling and epithelial-to-mesenchymal transition in human prostate cancer cells. *Cancer Res.* 2010;70:6735-6745.

33) Mani SA, Guo W, Liao MJ, *et al.* The epithelial-mesenchymal transition generates cells with properties of stem cells. *Cell* 2008;133:704-715.

34) Baiocchi M, Biffoni M, Ricci-Vitiani L, et al. New models for cancer research: human cancer stem cell xenografts. *Curr. Opin. Pharmacol.* 2010;10:380-384.

35) Kelly CM, Krishnamurthy S, Bianchini G, *et al.* Utility of oncotype DX risk estimates in clinically intermediate risk hormone receptor-positive, HER2-normal, grade II, lymph node-negative breast cancers. *Cancer.* 2010;116:5161-5167.

36) Hussain M, Smith MR, Sweeney C, *et al.* Cabozantinib (XL184) in metastatic castration-resistant prostate cancer (mCRPC): Results from a phase II randomized discontinuation trial. *J. Clin. Oncol* 2011:29 (suppl; abstr 4516).

37) Sequist LV, von Pawel J, Garmey EG, *et al.* Randomized phase II study of erlotinib plus tivantinib versus erlotinib plus placebo in previously treated non-small-cell lung cancer. *J. Clin. Oncol.* 2011;29:3307-3315.

38) Dai Y, Grant S. New insights into checkpoint kinase 1 in the DNA damage response signaling network. *Clin. Cancer Res.* 2010;16:376-383.

39) Zenvirt S, Kravchenko-Balasha N, Levitzki A. Status of p53 in human cancer cells does not predict efficacy of CHK1 kinase inhibitors combined with chemotherapeutic agents. *Oncogene* 2010;29:6149-6159.

40) Sausville EA, LoRusso P, Carducci MA, *et al.* Phase I dose-escalation study of AZD7762 in combination with gemcitabine (gem) in patients (pts) with advanced solid tumors. *J. Clin. Oncol.* 29: 2011 (suppl; abstr 3058).

41) Ho AL, Bendell JC, Cleary JM, *et al*. Phase I, open-label, dose-escalation study of AZD7762 in combination with irinotecan (irino) in patients (pts) with advanced solid tumors. *J. Clin. Oncol*. 29: 2011 (suppl; abstr 3033).

42) Daud A, Springett GM, Mendelson DS, *et al*. A phase I dose-escalation study of SCH 900776, a selective inhibitor of checkpoint kinase 1 (CHK1), in combination with gemcitabine (Gem) in subjects with advanced solid tumors. *J. Clin. Oncol*. 2010 ASCO Annual Meeting Proceedings (Post-Meeting Edition). Vol 28, No 15 suppl: 3064.

43) de Sousa EM, Vermeulen L, Richel D and Medema JP. Targeting Wnt signaling in colon cancer stem cells. *Clin. Cancer Res.* 2011;17:647-653.

44) Singh A and Settleman J. EMT, cancer stem cells and drug resistance: an emerging axis of evil in the war on cancer. *Oncogene* 2010;29:4741-4751.

45) Wilson A, Laurenti E, Oser G, *et al.* Hematopoietic stem cells reversibly switch from dormancy to self-renewal during homeostasis and repair. *Cell* 2008;135:1118-1129.

46) Dembinski JL, Krauss S. Characterization and functional analysis of a slow cycling stem cell-like subpopulation in pancreas adenocarcinoma. *Clin. Exp. Metastasis* 2009;26:611-623.

47) Gao MQ, Choi YP, Kang S, *et al.* CD24+ cells from hierarchically organized ovarian cancer are enriched in cancer stem cells. *Oncogene* 2010;29:2672-2680.

## 6) Figures

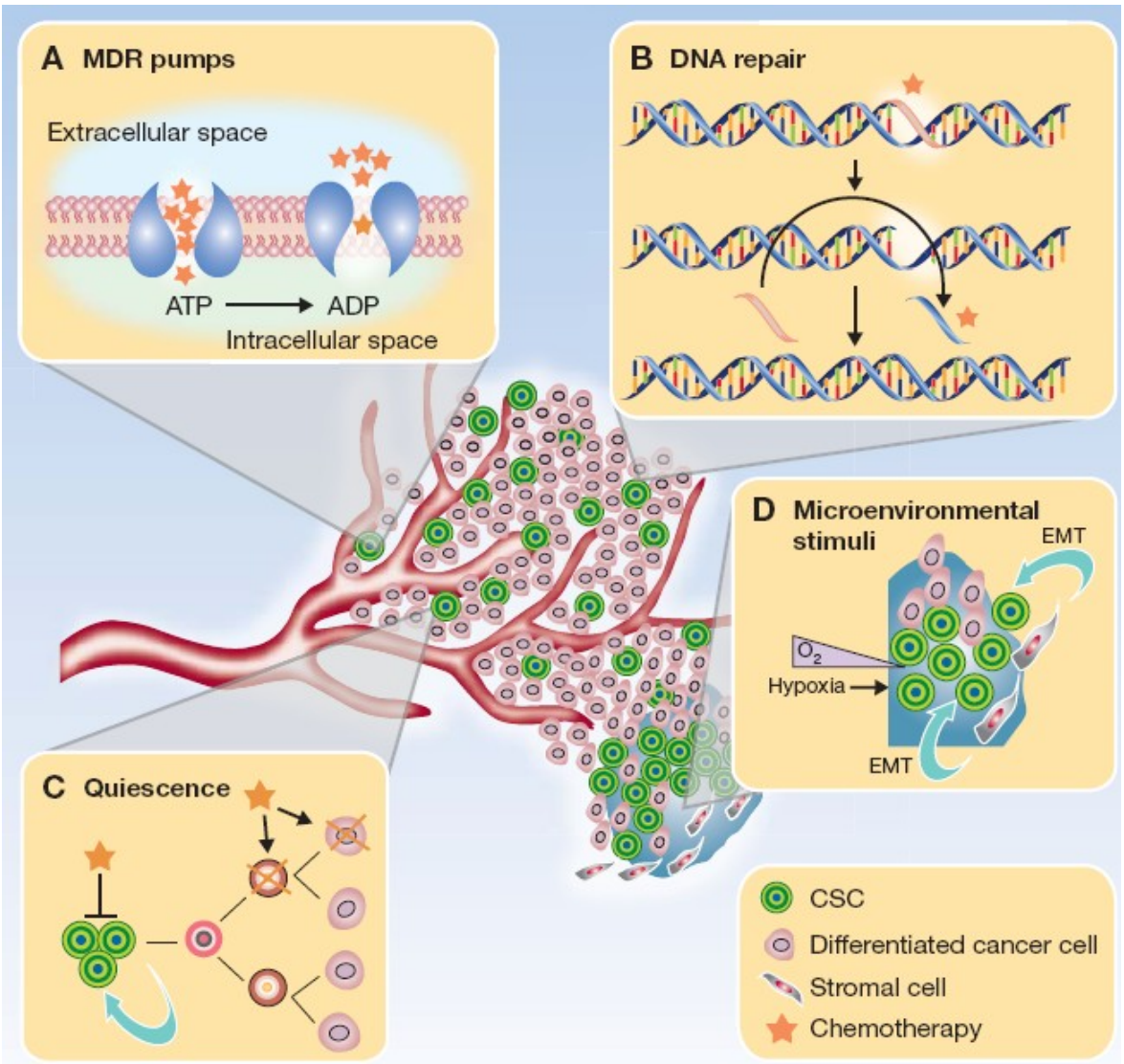


**Fig. 1: CSC-intrinsic (panel A,B,C) and CSC-extrinsic (panel D) mechanisms of chemoresistance**

| Sample | Age | Diagnosis | Receptor Status |
|---|---|---|---|
| BCSC#105 | 69 | Infiltrating Ductal Carcinoma | ER+ PR+ c-erbB2 + |
| BCSC#208 | 55 | Infiltrating Ductal Carcinoma | ER+ PR+ c-erbB2 + |
| BCSC#308 | 85 | Infiltrating Lobular Carcinoma | ER- PR- c-erbB2 - |
| BCSC#608 | 69 | Infiltrating Ductal Carcinoma | ER+ PR+ c-erbB2 - |
| BCSC#709 | 74 | Infiltrating Ductal Carcinoma | ER+ PR+ c-erbB2 + |
| BCSC#M | 72 | Infiltrating Ductal Carcinoma | ER+ PR+ c-erbB2 - |

Table1: breast cancer samples, patient demographics and specimen characteristics.

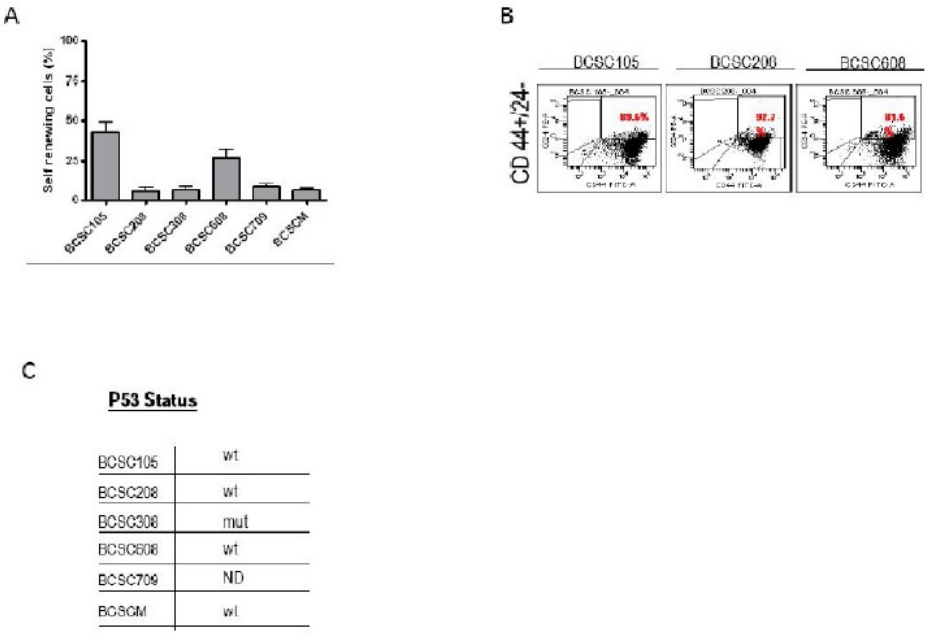


C

**P53 Status**

| | |
|---|---|
| BCSC105 | wt |
| BCSC208 | wt |
| BCSC308 | mut |
| BCSC608 | wt |
| BCSC709 | ND |
| BCSGM | wt |

Figure 2. Characterization of BCSC lines. A) Number of colonies obtained in soft agar assay under standard growth condition. Average number of colonies/plate for each BCSC lines. Mean ± SD of 3 independent experiments is shown. B) Flow cytometry analysis of three representative BCSC line double stained with CD24 PE and CD44 FITC. C) p53 mutation status evaluated in all 6 BCSC lines.

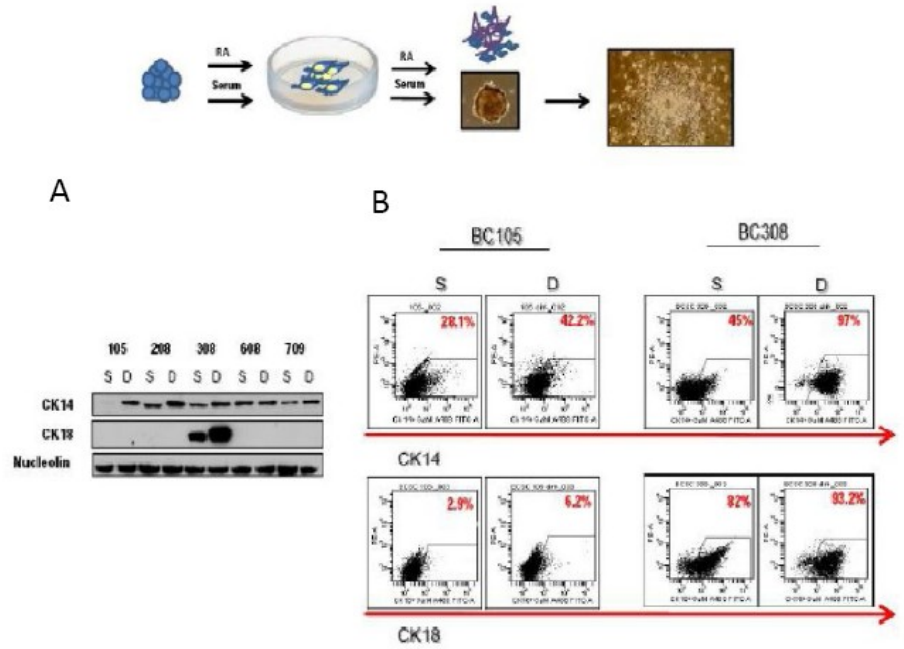


Figure 3. Serum-induced differentiation of BCSCs. A) Western blot analysis for CK14 and CK18 in BCSCs and differentiated progenies grown in the absence or in the presence of 5% FBS for 2 weeks. Nucleolin was used to assess equal loading. B) Flow cytometry analysis of BCSCs and differentiated progenies stained with CK18 and CK14.

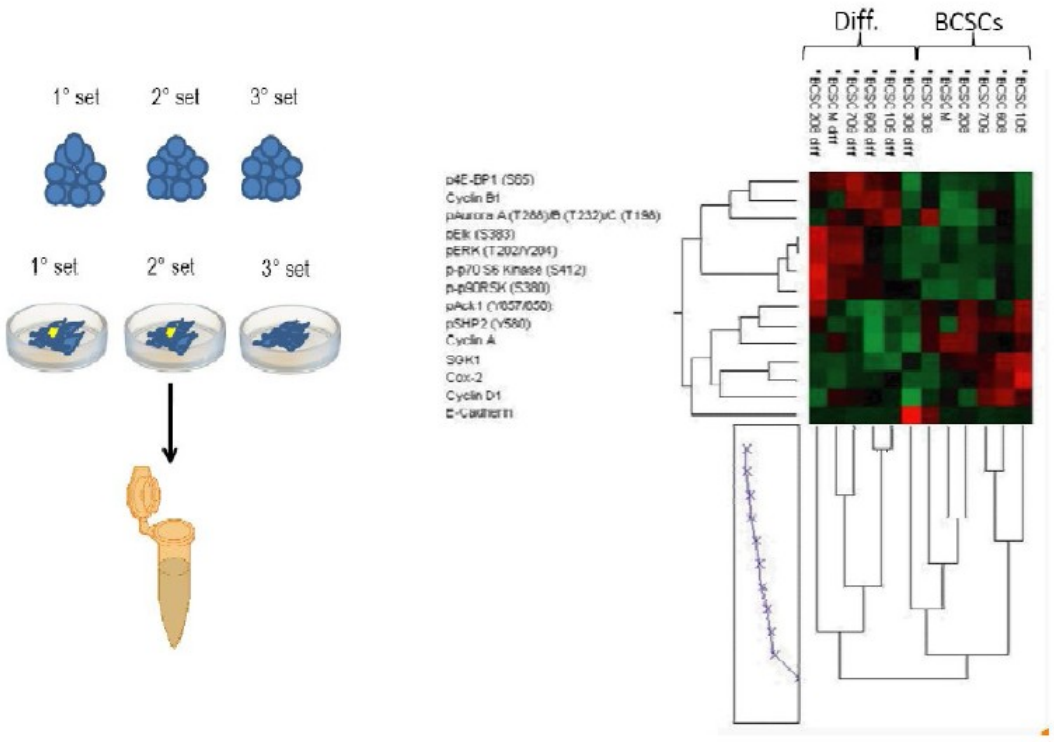


Figure 4. Reverse-Phase Protein Microarrays (RPPM) analysis. Hierarchical clustering of phosphoproteomic analysis performed on BCSCs *vs* differentiated counterparts obtained by analyzing three different sets of cell lysates obtained in distinct periods.

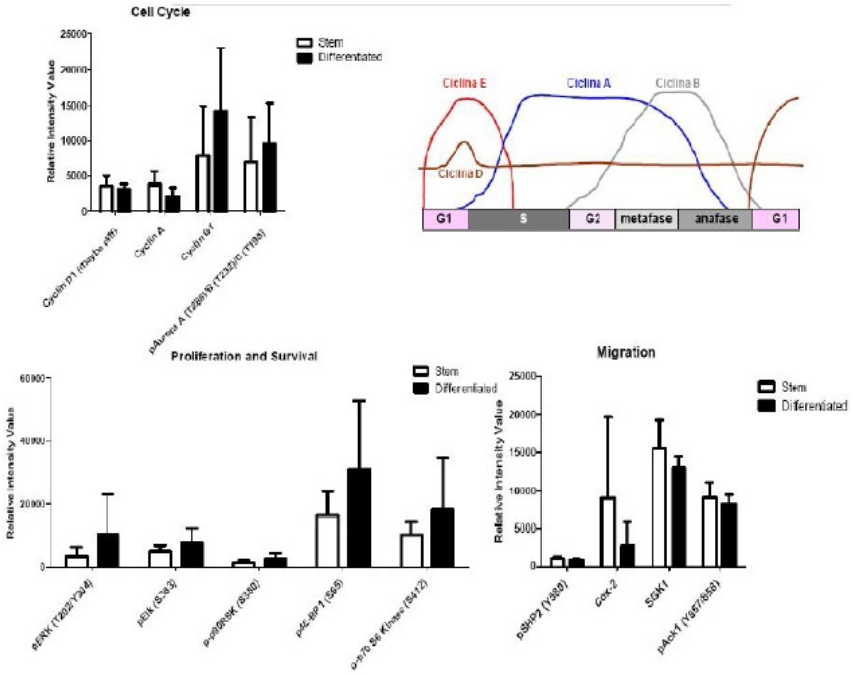


Figure 5. RPPM of BCSCs vs differentiated breast cancer cells. Graphical representation of signaling pathways activated in BCSCs over differentiated progeny.

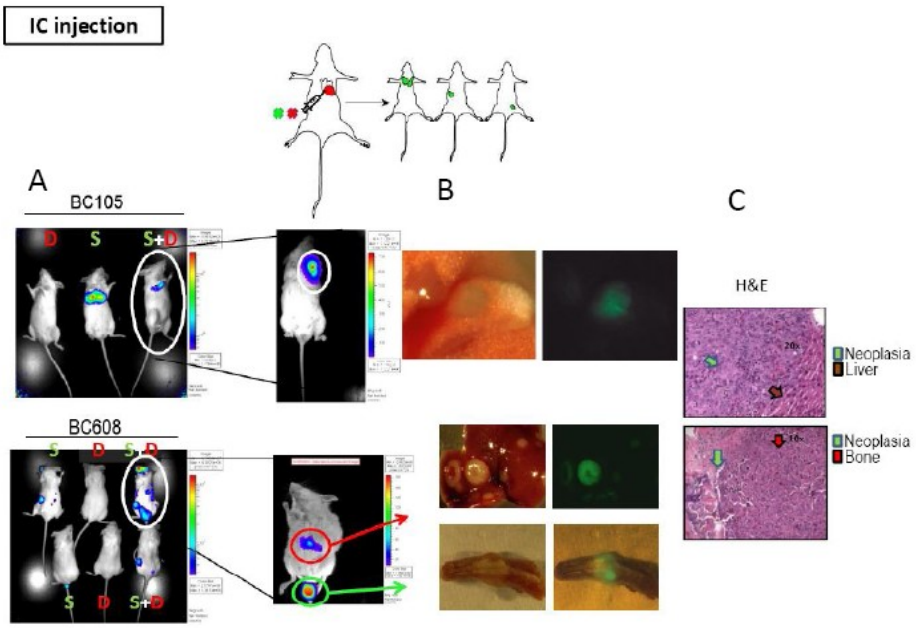


Figure 6. A) BCSCs (S) and differentiated (D) cells were transduced with lentiviral vectors coding for EGFP and RFP, respectively, and injected intracardiac (IC) alone or in a defined ratio. B) Representative image of breast cancer metastasis monitored with BLI and subsequently analyzed by stereomicroscopy. C) Representative H&E staining performed on fixed tissue indicating breast cancer metastases to the liver and to the bone of NOD-SCID mice.

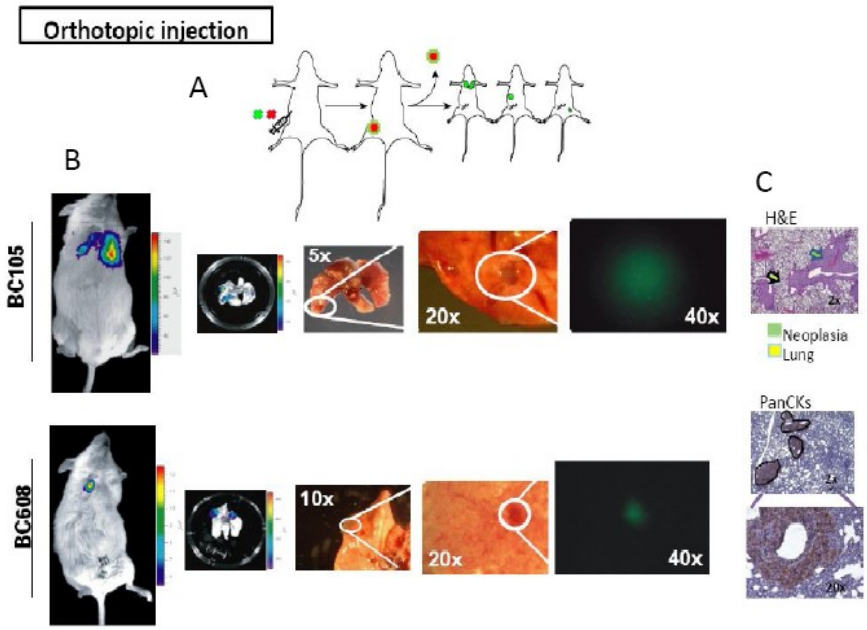


Figure 7. A) BCSCs (green) and differentiated cells (red) were orthotopically injected into the mammary fat pad of immunodeficient mice. Afterwards the primary tumors were removed and the onset of lung metastases was monitored. B) Representative image of breast cancer metastasis obtained following orthotopic injection monitored by bioluminescence imaging and analyzed by stereomicroscopy. C) Representative H&E and PanCKs staining preformed on fixed tissue indicating breast cancer metastasis to the lung of NOD-SCID mice.

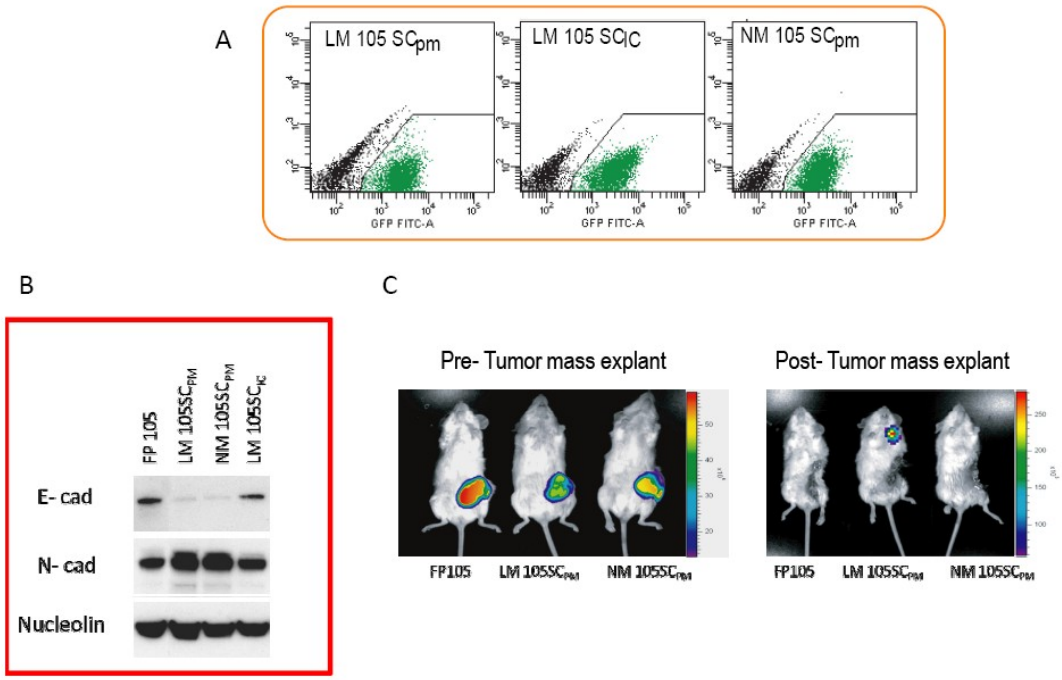


**Fig 8: A) GFP-sorted lung (LM105SCpm and LM105SCic) and nodal (NM105SCpm) metastases obtained after intracardiac and orthotopic injection, B) Expression of E-cadherin and N-cadherin on primary tumor (FP105) and metastases (LM105SCpm, NM105SCpm, LM105SCic), C) in-vivo *imaging* of the primary tumor and metastatic lesions.**

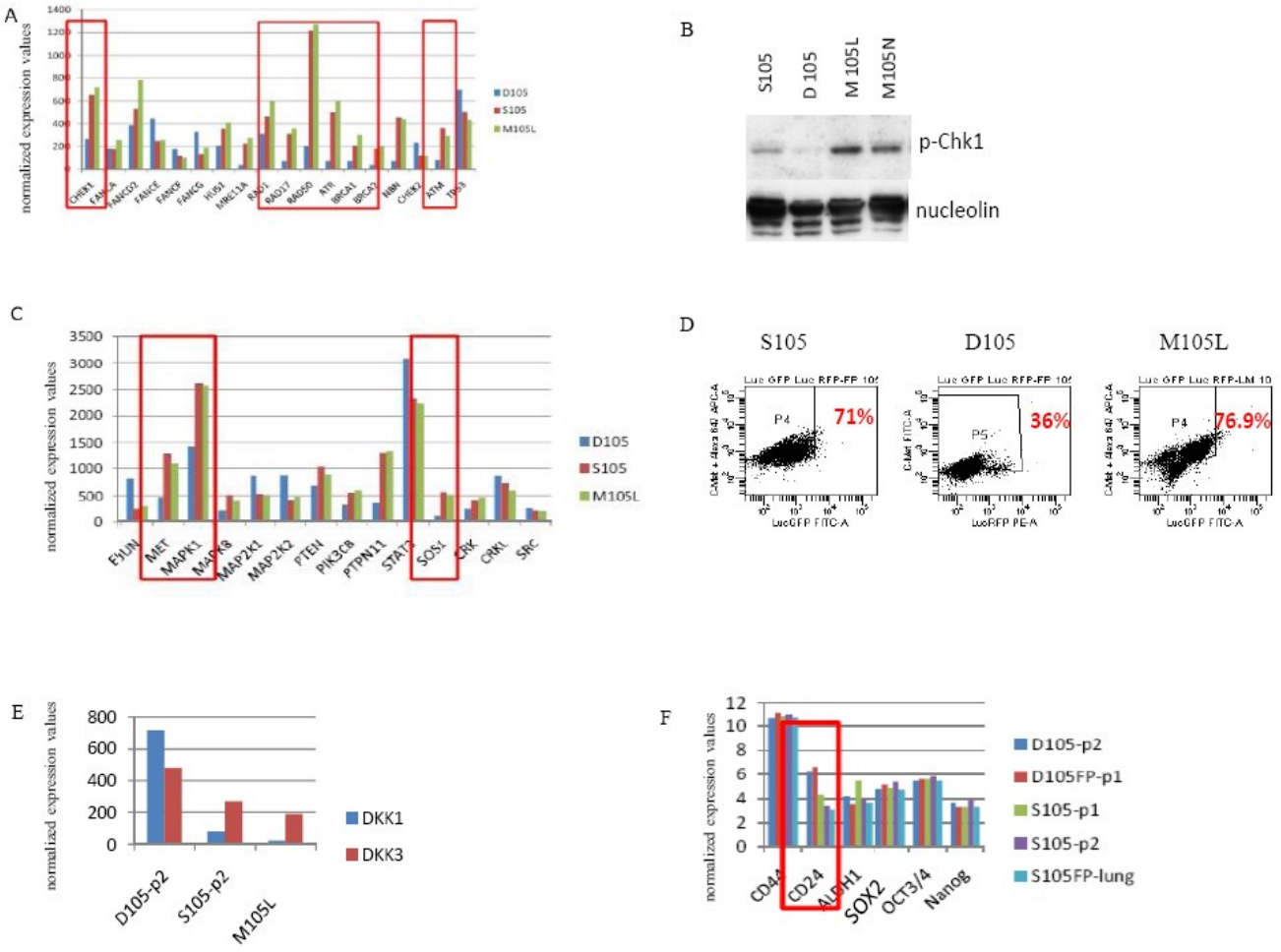


Fig. 9: A) Gene expression profiling showing an increased expression of ATM-Chk1 checkpoint effectors in BCSCs (S105 and M105L) compared with dBCCs (D105), B) increased levels of activated Chk1 in BCSCs (S105,M105L,M105N) confirmed by Western blot analysis, C) gene expression profiling showing an increased expression of c-Met pathway components in BCSCs (S105,M105L) compared with dBCCs (D105), D) FACS analysis confirming the differential c-MET expression, E) gene expression profiling showing reduced expression of the physiological Wnt pathway inhibitors DKK1 and DKK3 in BCSCs (S105p-2,M105L) and F) gene expression profiling showing the expression of established and putative cancer stem cell markers in BCSC- and dBCC-derived tumors.

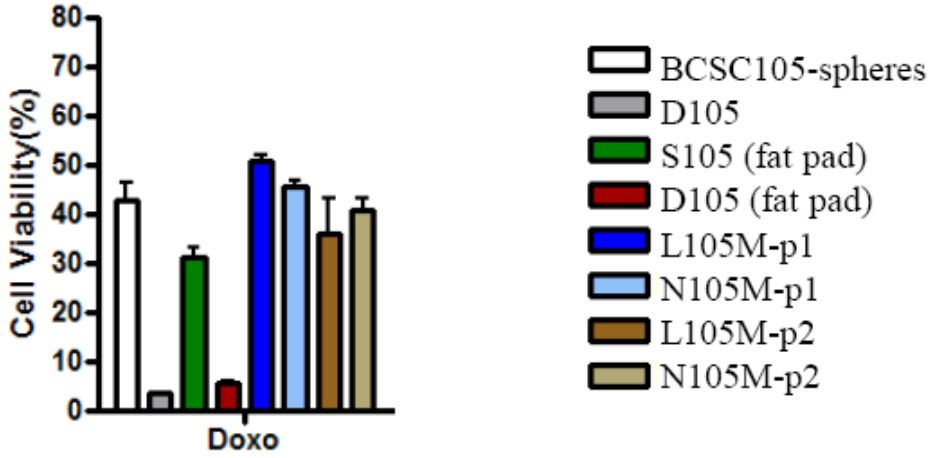


Fig. 10: enhanced chemoresistance of BCSCs and metastatic BCSCs compared to dBCCs